INTERNATIONAL SOCIETY FOR
SOIL MECHANICS AND
GEOTECHNICAL ENGINEERING

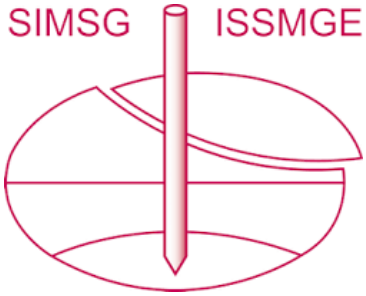

This paper was downloaded from the Online Library of the International Society for Soil Mechanics and Geotechnical Engineering (ISSMGE). The library is available here:

https://www.issmge.org/publications/online-library

This is an open-access database that archives thousands of papers published under the Auspices of the ISSMGE and maintained by the Innovation and Development Committee of ISSMGE.

The paper was published in the proceedings of the 6th International Conference on Geotechnical and Geophysical Site Characterization and was edited by Tamás Huszák, András Mahler and Edina Koch. The conference was originally scheduled to be held in Budapest, Hungary in 2020, but due to the COVID-19 pandemic, it was held online from September 26th to September 29th 2021.

Evaluation of Spatial Distribution for Permeability based on CPTU and Geostatistics

Shin-ichi Nishimura
Graduate School of Environmental and Life Science, Okayama University, Okayama, Japan, theg1786@okayama-u.ac.jp

Go Kubota[1], Toshifumi Shibata[2], Takayuki Shuku[3]
Graduate School of Environmental and Life Science, Okayama University, Okayama, Japan, pdvl1kbb@s.okayama-u.ac.jp[1], tshibata@cc.okayama-u.ac.jp[2], shuku@cc.okayama-u.ac.jp [3]

ABSTRACT: In this study, the spatial variability of the strength and permeability inside and underneath a river dike are addressed. Cone penetration tests (CPTUs) were conducted at the river dike site, which has piping histories. In addition, CPTUs were conducted in the laboratory as model tests on soil sampled from the river dike site, and permeability tests were also conducted on the same samples. Based on the laboratory tests, the relationship between the CPT results, which include the tip resistance, the side friction, and the pore pressure, and the permeability is derived. The relationship is applied to the in-situ test results. In conclusion, the spatial variability of the strength and permeability of the test site is evaluated with a geostatistical simulation technique.

Keywords: CPTU; spatial distribution; permeability; river dike; piping

1. Introduction

When heavy rains come, some river dikes breach. The two major causes of breaching are overflow and seepage failure due to piping. In this work, the procedure for detecting the locations that could be at high risk for piping inside the dikes or in their underlying layers is discussed to mitigate the risk.

Although boring and standard penetration tests are usually conducted to examine the inside of soil structures, the interval of the test points must be sparse due to low efficiency and in order to avoid damage to the structures. Consequently, weak locations may be overlooked. To deal with these shortcomings, the cone penetration test (CPTU) is used to obtain detailed information on the inside of the dikes or underneath them. The CPTU is advantageous in that it makes short-interval exams possible, due to its high efficiency, and it causes little damage to the structures.

To detect the locations of piping risk, the distribution of permeability in the ground must be identified. The relationship between the CPTU results and the coefficients of permeability is derived to evaluate the in-situ permeability by CPTUs. For this task, model CPTUs and permeability tests were conducted with the same soil samples. A regression equation was derived that represents the relationship of the permeability and the CPTU results, namely, the tip resistance, and the side friction.

Some previous articles have addressed the permeability derived from CPTUs. For example, Robertson (2010)[1] presented the relationship between CPT results and the permeability. Wang and Tong (2014) [2] also predicted the permeability with CPTUs and a similar concept. Paradis *et al*. (2014)[3] used CPTUSMR, and determined the spatial variability of the permeability.

The present study also deals with the spatial variability of the permeability. Firstly, a statistical model is determined from the CPTU results to present the spatial distribution of the permeability. Secondly, the permeability inside and underneath a river dike is spatially interpolated by a geostatistical simulation.

1. Field investigation

1.1. Cone penetration tests (CPTUs)

In the CPTUs, tip resistance q_t, side friction f_s, and pore water pressure P_w are measured. Robertson and Fear (1995)[4] proposed a type of soil behavior index, I_c, based on q_t and f_s, which is defined by Eq. (1), as follows:

$$I_c = \left\{ \left(3.47 - \log Q_t\right)^2 + \left(1.22 + \log F_R\right)^2 \right\}^{0.5} \quad (1)$$

$$Q_t = \left(q_t - \sigma_{v0}\right) / \sigma'_{v0} \quad (2)$$

$$F_R = f_s / \left(q_t \quad _{v0}\right) \quad (3)$$

in which Q_t is the generalized tip resistance, σ_{vo} is the vertical total stress, σ_{vo}' is the vertical effective stress, and F_R is the generalized side friction ratio (Robertson, 1990)[5].

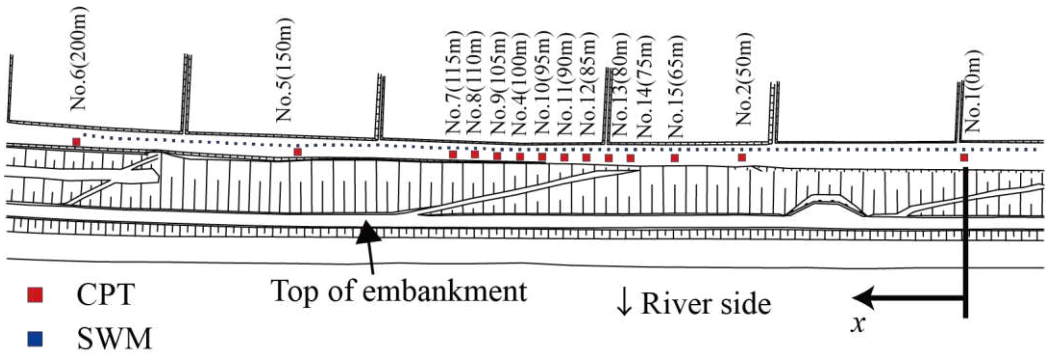

Figure 2. Plan of investigation site.

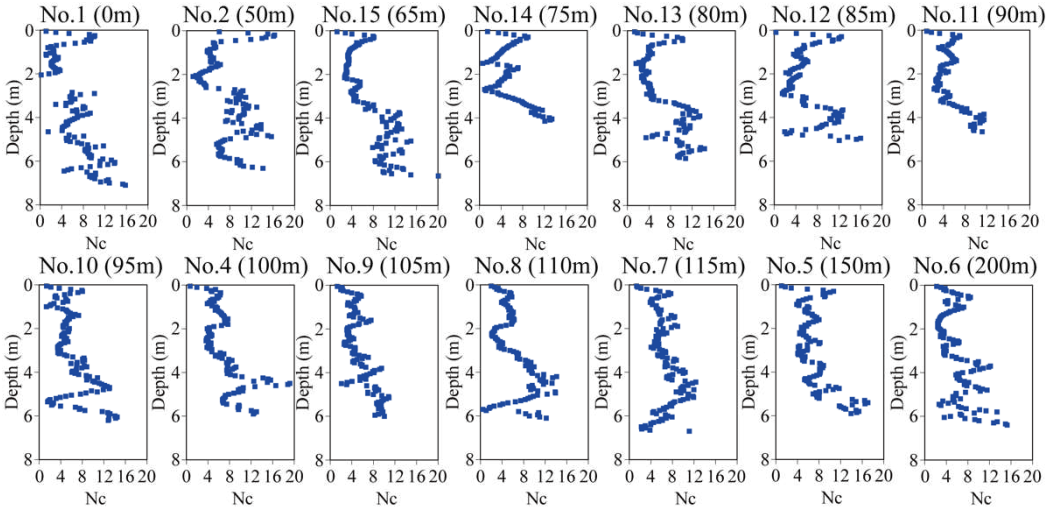

Figure 3. N values distribution derived from CPTs at Oda River site.

Suzuki *et al*. (2003) [6] proposed the transformation equation from I_c and q_t to the CPT N value, N_c, as follows:

$$N_c = 0.341 I_c^{1.94} \left(q_t \quad 0.2\right)^{\left(1.34 \quad 0.0927 I_c\right)} \quad \left(q_t > 0.2\text{MPa}\right)$$
$$N_c = 0 \quad \left(q_t \quad 0.2\text{MPa}\right) \qquad (4)$$

The relationship between N_c and the N value of the standard penetration tests, N_{SPT}, is based on the data obtained from embankment sites; it is presented in Fig.1. Since the embankment sites have relatively low N values, in the range of 0-10, Eq.(5) is defined based on Fig.1. Transformation error ε_r is also evaluated.

$$N_{SPT} = N_c(1+0.62 \quad _r) \qquad (5)$$

1.2. Outline of site

A site investigation was conducted on the Oda River dike in Okayama, Japan. A 200-m span along the dike axis was examined, as depicted in Fig.2. As the first step, CPTUs were conducted at long intervals of 50 m. As the second step, sounding tests were conducted at short intervals of 5 m. Short-interval tests are definitely required to determine the geostatistical parameters, namely, the lateral correlation lengths.

1.3. CPTU results

In Fig.3, the results of the CPTUs are given, namely, the CPT N-values, N_c. According to the figure, there are soft layers at depths around 2 m and 5.5 m. Below the depth of 7 m, the ground is composed of stiff gravel and a sand layer; this does not affect the instability of the dike.

In Fig.4, the soil classification is given. The whole area is dominated by the sand layer. Layers of clay or sandy mixtures are found around the depth =1~2.5 m in the lateral range of x=0~50 m, and around the depth 6 m, in the lateral range of x=100~150m, while layers of silty and sandy mixtures are found around the depth 6.0 m at x=200 m.

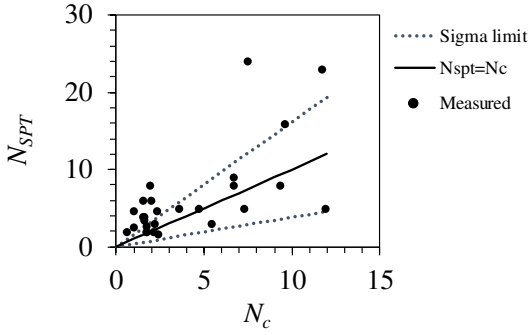

Figure 1. Relationship between N_{spt} and N_c.

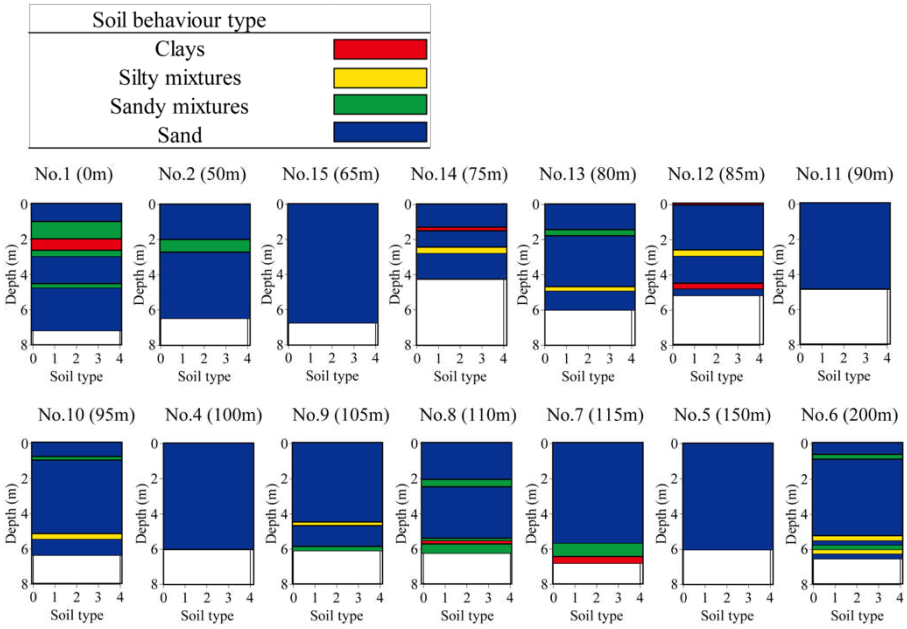

Figure 4. Soil classification derived from CPTs at Oda River site.

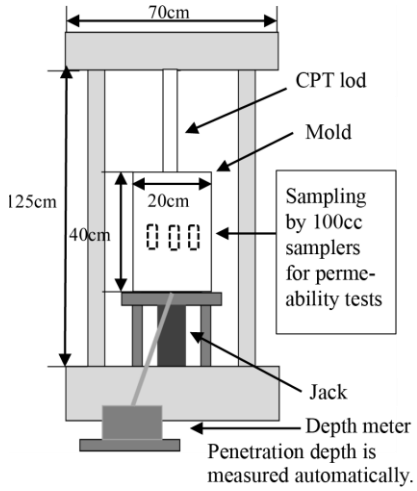

Figure 5. Model test equipment.

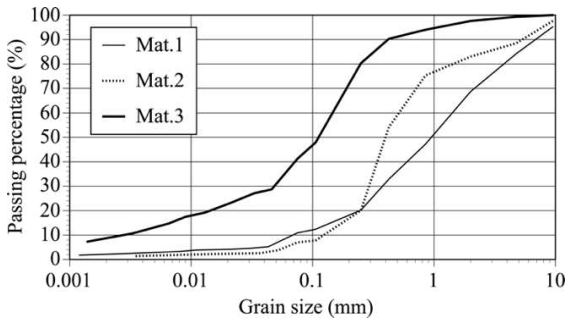

Figure 6. Grain size distribution.

2. Model CPTUs and permeability tests

2.1. Test materials and equipment

To create the relationship between the CPTU results and the permeability, model CPTUs and permeability tests were conducted simultaneously. Fig.5 shows the testing equipment. After the sampled soils are compacted in the mold, the CPTUs are conducted. From the compacted soil, the soil specimens are cut out by the 100-cc samplers for the permeability tests. In conclusion, the q_t, f_s, and p_w values are obtained by the model CPTUs, and the permeability is obtained by the permeability tests from the same samples.

The materials are sampled from the Oda River site, where piping phenomena have been observed several times due to heavy rains. The grain size distributions are depicted in Fig.6. The three materials, Mats. 1, 2, and 3, have different distributions. Mat. 1 is the finest, while Mat. 3 is the coarsest.

2.2. Test results

Mat. 1 is compacted into three degrees of compaction, and the effect of the unit weights is clarified. The initial water content of all the specimens was set to 10%. Table 1 presents the test cases and results.

Fig.7 presents an example of the tests. The Figs.6(a) and (b) are the tip resisttance and the side friction, and the almost constant values are measured with the depth. The pore water pressures, however, could not be measured reasonably, since the samples were in the usaturated state.

According to the test results, in cases where the unit weights are almost the same, the permeability increases in the order of Mat. 2, Mat. 3, and Mat. 1. The results correspond to the grain size distributions of the materials. As for the different degrees of compaction, the greater

the unit weight of the specimen, the greater the corresponding tip resistance and the smaller the permeability.

From these results in Table 1, permeability k is derived by Eq.(6).

$$\begin{aligned}\log k = & \ 4.91 \quad 6.85 \quad 10^{-5} q_t \\ & 1.43 \quad 10^{-2} f_s \quad 5.76 \quad 10^{-9} q_t^2 \\ & +1.11 \quad 10^{-5} f_s^2 + 2.68 \quad 10^{-6} q_t f_s\end{aligned} \tag{6}$$

where the unit of k is m/s, and the unit of tip resistance q_t and side friction f_s is kPa.

Since the degree of saturation in the conducted test cases is low, and the sensitivity of p_w is supposed to be low, Eq.(6) does not include the pore water pressure. The second order regression equation is employed here, since the relatively low order regression is favorable to obtain the mild trend in the extrapolation

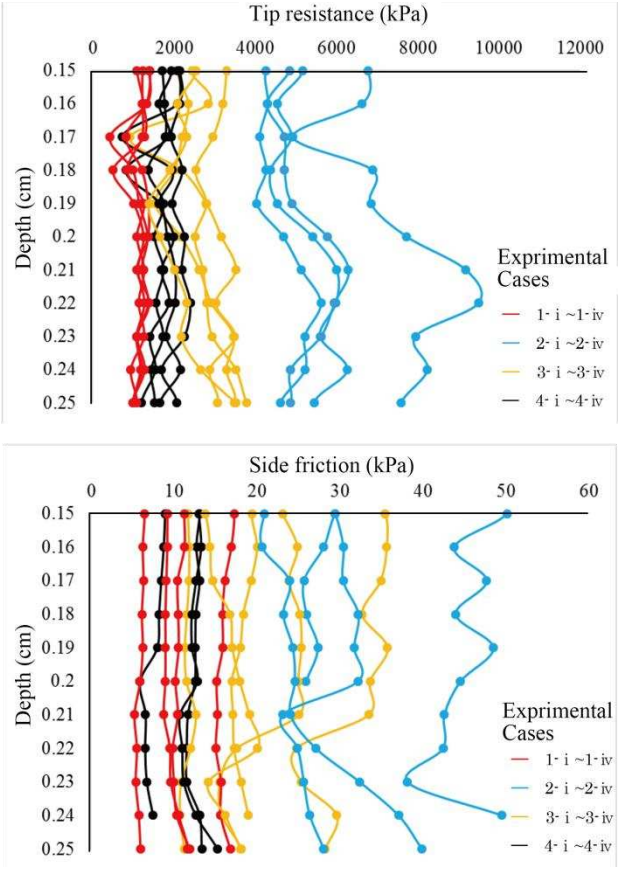

Figure 7. Examples of measured tip resisanses and side frictions.

Table 1. Experimental cases and results of CPTUs and permeability.

Test Num.	k [m/s]	qt [kPa]	fs [kPa]	pw [kPa]	ρt [g/cm^3]	e	Sr [%]	w [%]
1- i	1.35E-05	1129.0	11.9	-0.154	1.76	0.649	39.2	9.60
1- ii	1.34E-05	1208.1	18.9	0.111	1.76	0.658	40.0	9.93
1- iii	8.66E-06	1087.7	10.5	-0.245	1.76	0.655	39.3	9.72
1- iv	1.08E-05	1135.8	6.3	0.582	1.75	0.664	40.4	10.13
2- i	5.20E-06	5295.4	35.2	0.263	1.95	0.509	58.5	11.25
2- ii	3.46E-06	7478.6	65.4	4.704	1.96	0.511	61.2	11.80
2- iii	3.90E-06	5171.7	37.6	0.170	1.96	0.573	76.8	12.92
2- iv	6.50E-06	4679.8	35.2	2.088	1.96	0.487	55.5	10.21
3- i	4.33E-06	2559.1	27.1	-0.409	1.91	0.536	52.6	10.66
3- ii	2.60E-06	3005.7	42.7	0.521	1.92	0.525	53.0	10.52
3- iii	3.75E-06	2757.7	22.2	0.021	1.93	0.511	51.4	9.92
3- iv	3.68E-06	2230.1	19.7	0.747	1.84	0.610	51.2	11.80
4- i	4.87E-06	1760.3	14.4	-0.606	1.83	0.595	44.6	10.02
4- ii	4.33E-06	1657.6	8.2	0.903	1.83	0.583	41.8	9.20
4- iii	3.90E-06	1622.6	13.1	0.101	1.80	0.630	44.4	10.56
4- iv	8.23E-06	2105.6	14.2	0.428	1.80	0.625	43.4	10.24
5- i	3.81E-05	6612.1	160.1	-0.485	1.72	0.726	43.0	11.60
5- ii	3.12E-05	8074.0	162.4	0.244	1.72	0.700	41.7	10.85
5- iii	3.64E-05	6731.8	131.8	-0.048	1.79	0.706	33.9	8.88
5- iv	3.12E-05	8178.5	165.4	-2.597	1.77	0.706	44.7	11.72
6- i	3.46E-06	5224.1	121.3	0.170	1.74	0.689	29.1	7.44
6- ii	3.90E-06	5452.5	141.0	0.682	1.76	0.687	28.8	7.34
6- iii	4.33E-06	4010.1	73.8	1.090	1.72	0.635	35.1	8.25
6- iv	2.17E-06	4292.3	102.3	-0.475	1.76	0.645	32.8	7.84

Test numbers 1, 2, 3, and 4: Mat. 1; Test number 5: Mat. 2; Test number 6: Mat. 3.
The Roman numbers are the repeat numbers.

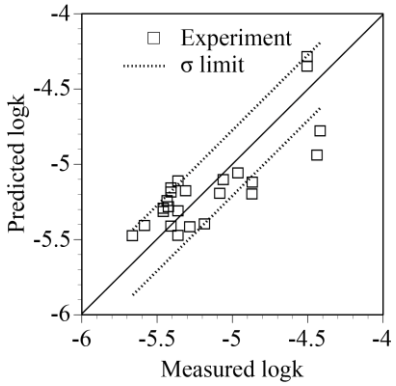

Figure 8. Relationship between measured and predicted permeabilities.

range of the variables. While. the q_t and f_s have the correlation, and therefore, the term $q_t f_s$ should be included, and second order regression is selected as Eq.(6) rather than the linear function.

Fig.8 depicts the relationship of the measured permeability and that predicted by Eq.(6). The figure shows that the correspondence between the measured and the predicted permeabilities is relatively good. Transformation error ε_k is added to log$k$ and the transformed permeability, k_T, can be evaluated by Eq.(7).

$$\log k_T = \log k + \quad _k \ _k \tag{7}$$

in which σ_k=0.246 is the standard deviation depicted in Fig.8 as the σ limit, and ε_k is the N(0,1) type of normal random variable.

2.3 Application to field test results

The log k, derived from the in-situ CPT results by Eq.(6), is presented in Fig.9. Around the locations of x = 50, 85, and 150 m of z= 0~0.4 m, the permeability is very high. At x =100 and 150 m of around z=5 m, there are also high permeability zones.

3. Statistical methods

3.1. Statistical models of spatial variability

A representative variable for the soil properties, s, which corresponds to logN_c or log$k$ in this study, is defined by Eq.(8) as a function of location $\mathbf{X}$=(x, y, z). Variable s is assumed to be expressed as the sum of mean value m and random variable U, which is a normal random variable in this study.

$$s(\mathbf{X}) = m(\mathbf{X}) + U(\mathbf{X}) \tag{8}$$

The random variable function, $s(\mathbf{X})$, is discretized spatially into random vector $\mathbf{s}^t$=(s_1,s_2,...,s_M), in which s_k is a point estimation value at location $\mathbf{X}$=(x_k, y_k, z_k). The soil parameters, which are obtained from the tests, are defined here as $\mathbf{S}^t$=(S_1,S_2,..., S_M). Symbol M signifies the number of test points. Vector $\mathbf{S}$ is considered to be the realization of random vector $\mathbf{s}^t$=(s_1,s_2,...,s_M). If variables s_1, s_2,..., s_M constitute the M - variate normal distribution, the probability density function of the variable, s can then be given by the following equation:

$$f_S(\mathbf{s}) = (2\ )^{\frac{M}{2}} |\mathbf{C}|^{\frac{1}{2}} \exp\left\{ \frac{1}{2}(\mathbf{s}\quad \mathbf{m})^t \mathbf{C}^{\ 1}(\mathbf{s}\quad \mathbf{m}) \right\} \tag{9}$$

in which $\mathbf{m}^t$=(m_1,m_2,...,m_M) is the mean vector of random vector $\mathbf{s}^t$=(s_1,s_2,...,s_M); it is assumed to be the following regression function. In this research, a 2-D statistical model is considered, namely, horizontal coordinate x, which is parallel to the embankment axis, and vertical coordinate z are introduced here. The element of the mean vector is described as

$$m_k = a_0 + a_1 x_k + a_2 z_k + a_3 x_k^2 + a_4 z_k^2 + a_5 x_k z_k \tag{10}$$

in which (x_k, z_k) means the coordinate corresponding to the position of parameter s_k, and a_0, a_1, a_2, a_3, a_4, and a_5 are the regression coefficients.

C is the M×M covariance matrix, which is selected from the following four types in this study:

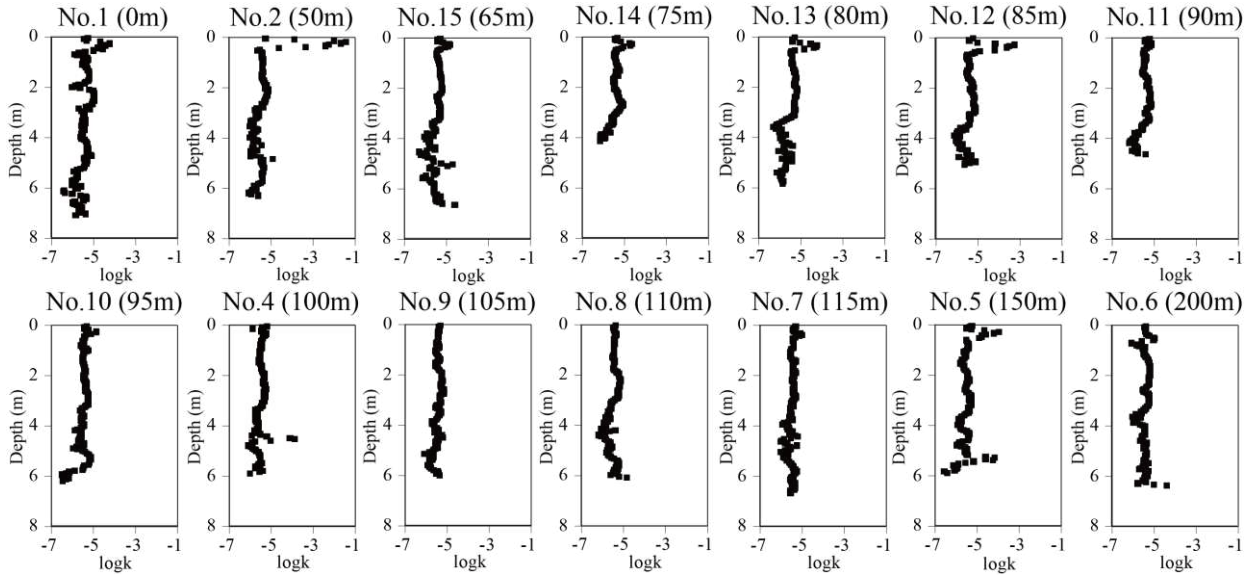

Figure 9. Permeability derived from CPTUs at Oda River site.

$$\mathbf{C}=\left[C_{ij}\right]$$

$$=\begin{cases}\sigma^2\exp\left(-\dfrac{\left|x_i-x_j\right|}{l_x}-\dfrac{\left|z_i-z_j\right|}{l_z}\right) & \text{(a)}\\ \sigma^2\exp\left\{-\dfrac{\left(x_i-x_j\right)^2}{l_x^2}-\dfrac{\left(z_i-z_j\right)^2}{l_z^2}\right\} & \text{(b)}\\ \sigma^2\exp\left\{-\sqrt{\dfrac{\left(x_i-x_j\right)^2}{l_x^2}+\dfrac{\left(z_i-z_j\right)^2}{l_z^2}}\right\} & \text{(c)}\\ N_e\sigma^2\exp\left(-\dfrac{\left|x_i-x_j\right|}{l_x}-\dfrac{\left|z_i-z_j\right|}{l_z}\right) & \text{(d)}\end{cases} \tag{11}$$

$$i,j=1,2,\cdots,M$$

$$\begin{cases}N_e=1 & (i=j)\\ N_e\le 1 & (i\ne j)\end{cases}$$

in which the symbol $[C_{ij}]$ signifies an i-j component of the covariance matrix, σ is the standard deviation, and l_x, and l_z are the correlation lengths for the x and z directions, respectively. Parameter N_e is related to the nugget effect. Akaike's Information Criterion, AIC (Akaike, 1974)[7], is defined by Eq.(12) considering the logarithmic likelihood.

$$\begin{aligned}\mathrm{AIC}=\ & 2\times\max\left\{\ln f_S(\mathbf{S})\right\}+2L=M\ln 2\\ &+\min\left\{\ln|\mathbf{C}|+(\mathbf{S}\quad\mathbf{m})^t\,\mathbf{C}^{-1}(\mathbf{S}\quad\mathbf{m})\right\}+2L\end{aligned} \tag{12}$$

in which L is the number of unknown parameters included in Eq.(9). By minimizing AIC (MAIC), the regression coefficients of the mean function, the number of regression coefficients, the standard deviation, σ, a type of covariance function, the nugget effect parameter, and the correlation lengths are determined. In other words, the determined parameters and the selected covariance function correspond to the minimum AIC.

For logN_c and log$k$, the determined mean and covariance functions are determined by the following equations, respectively:

logN_c:

$$m=0.379+0.111z \tag{13}$$

$$C(\Delta x,\Delta z)=(0.261)^2\exp\left\{-\sqrt{\left(\frac{\Delta x}{10.0}\right)^2+\left(\frac{\Delta z}{0.48}\right)^2}\right\} \tag{14}$$

log$k$:

$$m=-5.23-0.0557z \tag{15}$$

$$C(\Delta x,\Delta z)=(0.476)^2\exp\left\{-\sqrt{\left(\frac{\Delta x}{15.9}\right)^2+\left(\frac{\Delta z}{0.46}\right)^2}\right\} \tag{16}$$

3.2. Geostatistical simulation method

In the present study, the sequential Gaussian simulation method is conducted; analysis code SGSIM (Deutsch and Journel 1992)[8] is employed for the task. A realization $\xi_c^{(l)}$ by SGSIM is given by Eq.(17); it is conditioned at the sample points so that the realized values coincide with the sample values.

$$\xi_c^{(l)}(x,z)=\quad(x,z)+\ ^{(l)}(x,z)\qquad^{(l)}(x,z) \tag{17}$$

in which $\xi_c^{(l)}(x,z)$ means that the l th realization, $\xi^*(x,z)$, is an estimated value by kriging, and $\xi^{(l)}(x,z)$ is the l th realization without conditioning. $\xi^{*(l)}(x,z)$ is the kriged estimation using the values of $\xi^{(l)}(x,z)$ at the sampling points. On the right side of Eq.(17), the first item is an estimated value of kriging as an average. The remainder of the second and third items shows an estimation error of kriging. The realization, $\xi_c^{(l)}(x,z)$ is used as logN_c and log$k$. To the generated realizations of N_c, and log$k$, the transformation errors are added, and finally, random numbers for N_{SPT} and logk_T are created. For the random variables, the Monte Carlo simulation is repeated 2000 times.

4. Results of simulations

4.1. Spatial distribution of N values

Fig.10 shows the distribution of N_{SPT} interpolated by the geostatistical simulation. Figures (a), (b), and (c) present the mean, the standard deviation, and the probability of N < 5, respectively. Weak locations are found around x=0~30 m, z=1.5~3.0 m; x=180~210 m,

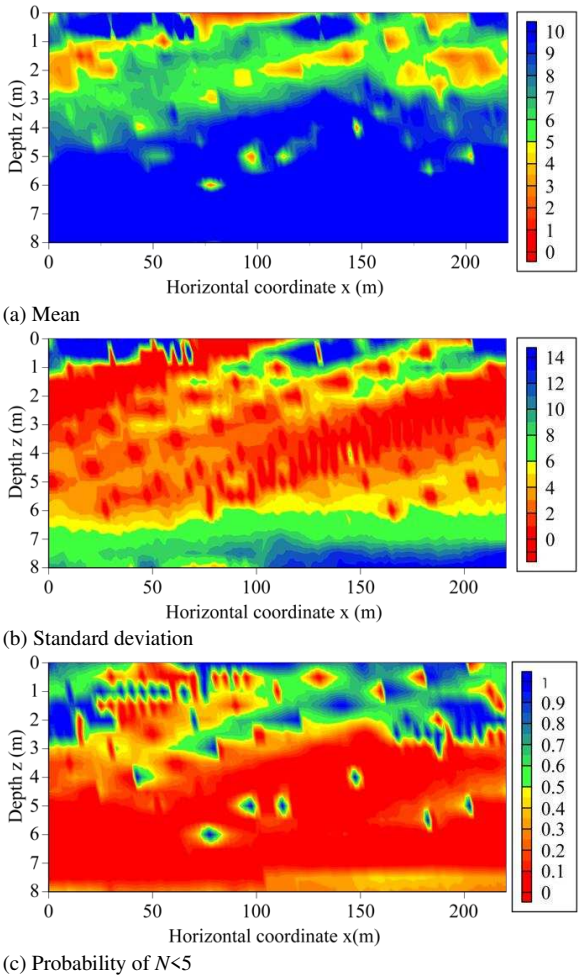

Figure 10. Simulation results for N_{SPT}

z=1.5~3.0; and x=70~120 m, z=0.0~0.3 m. Except for the span at x=30~100 m, around z=1~3 m, there are weak locations.

4.2. Spatial distribution of permeability

Figs.11(a) and 9(b) present the mean and the standard deviation of transformed permeability k_T. The trend of the two figures is coincidental. At locations of (x m, z m) = (0~40, 0~3), (0~40, 4.5~5.5), (130~180, 0~0.5), (170~190, 1.5~3.5), and (170~190, 4.0~6.5), the possibility of high permeability is great. Considering Fig. 8(c), the permeability is high and the strength is low at the locations of (x m, z m) =(0~30, 1.5~3) and (180~190, 1.5~3.0). The piping risk is also supposed to be high at these locations.

5. Conclusions

(1) As a field investigation approach, CPTUs were conducted with the long intervals of 50 m, namely, the tests were sparsely conducted. According to the results of the sparse tests, detailed tests with short intervals of 5 m were then scheduled. Based on the detailed tests, it was possible to precisely predict the weak locations and to determine the parameters for the geostatistical modeling.

(2) To confirm the relationship between the CPT results and the coefficients of permeability, model CPTUs and permeability tests were conducted with the same samples. The relationship between the measured permeability and that predicted by the CPTUs was derived.

(3) The statistical models used to present the spatial variability for the N value and the permeability were reasonably determined from the CPT results.

(4) As a spatial interpolation method, a sequential Gaussian simulation was employed. With this approach, the weak locations (N <5) and the highly permeable areas were identified. These areas could be at high risk for piping.

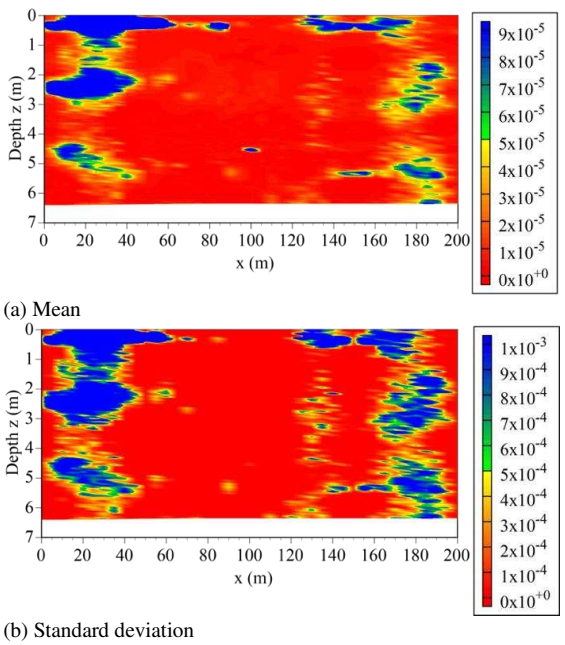

Figure 11. Simulation results for k_T (Unit: m/s)

References

[1] Robertson P.K. "Estimating in-situ soil permeability from CPT and CPTu", 2nd International Symposium on Cone Penetration Testing, Huntington Beach, CA, USA., 2010.

[2] Wang, Q., Tong, L. " Determination permeability coefficient from piezocone", *Advances in Materials Science and Engineering*, Vol. 2014, Article ID 396428., 2014.

[3] Paradis, D., Lefebvre, R., Gloaguen, E., Rivera A. "Predicting hydrofacies and hydraulic conductivity from direct-push data using a data-driven relevance vector machine approach: Motivations, algorithms, and application", WRR, 51, pp. 481-505, 2014.

[4] Robertson, P.K., Fear, C. E. " Liquefaction of sand and its evaluation", Proc. of 1st. Int. Nat. Symp. on Earthquake Geotechnical Engineering, IS-Tokyo'95, Vol. 3, pp. 1253-1289, 1995.

[5] [5] Robertson, P. K. " Soil classification using the cone penetration test", Canadian Geotechnical Journal, 28(1), pp. 151-158, 1990.

[6] Suzuki, Y., Tokimatsu, K., Sanematsu, T. " Correlations between CPT data and soil characteristics obtained from SPT", *J. Struct. Constr. Eng.*, AIJ, No. 566, pp. 73-80, 2003.

[7] Akaike, H. "A new look at the statistical model identification", IEEE Trans. on Automatic Control, AC-19(6), pp. 716-723, 1974.

[8] Deutsch, C. V. and Journel, A. G. *Geostatistical Software Library and User's Guide*, Oxford University Press., 1992.